Lattice gas model of coherent strained epitaxy

V. I. Tokar[1,2] and H. Dreyssé[1]
[1]*IPCMS-GEMM, UMR 7504 CNRS, 23 rue du Loess, F-67034 Strasbourg Cedex, France*
[2]*Institute of Magnetism, National Academy of Sciences, 36-b Vernadsky str., 03142 Kiev-142, Ukraine*
(Received 12 May 2003; revised manuscript received 1 August 2003; published 24 November 2003)

The harmonic Frenkel-Kontorova model is used to illustrate with an exactly solvable example a general technique of mapping a coherently strained epitaxial system with continuous atomic displacements onto a lattice gas model (LGM) with only discrete variables. The misfit strain of the original model is transformed into cluster interatomic interactions of the LGM. In the case of rectangular geometry the clusters are contiguous atomic chains of all lengths, but the interaction strength for long chains is exponentially small. This makes possible the application of efficient Monte Carlo techniques for discrete variables both in kinetic and equilibrium studies. The formalism developed can be applied to one- and two-dimensional systems but as an illustrative example, we consider only the problem of self-assembly of one-dimensional size calibrated clusters on the steps of vicinal surfaces. In this case the model can be solved exactly. Besides the size calibration at zero temperature, the solution exhibits a new phenomenon of transient self-assembly. The latter consists in the appearance at intermediate temperatures of self-assembled clusters with their mean size growing at lowering temperature. The phenomenon is caused by the forces due to the entropy of atomic displacements.

DOI: 10.1103/PhysRevB.68.195419 PACS number(s): 68.65.−k, 81.07.−b, 81.16.Dn

I. INTRODUCTION

The phenomena of self-assembly and self-organization of coherent (i.e., dislocation-free) size calibrated nano- and atomic-scale structures observed during the heteroepitaxial growth in some systems[1,2] are considered to be promising tools for fabrication of microelectronic devices.[3]

A major factor influencing the phenomenon of self-assembly is the lattice size misfit between the substrate and the growing overlayer which is usually encountered in heteroepitaxial systems.[4] The misfit strain is believed to be the driving force behind the size calibration.[4,5] So its adequate description should lie at the basis of any theory of strained epitaxy. Because strained systems exhibit complicated kinetics and morphologies, analytical approach is difficult in most cases, so a major technique in theoretical studies of strained epitaxy is the kinetic Monte Carlo simulation. The application of this technique, however, is severely hampered by the necessity to simulate the continuous atomic displacements which is much more difficult a task than simulation of discrete variables.[6] Therefore, atomistic models in such simulations are currently restricted to rather small systems consisting of only a few thousand atoms[7] while experimentally observed three-dimensional (3D) quantum dots sometimes consist of several tens of thousand atoms each.[2]

The present study is based on the observation that as long as we are interested only in *coherent* structures, there is a possibility to map the system onto a purely lattice model. Irrespective of how strongly a coherent structure is deformed, in the absence of dislocations there always exists a lattice site of a regular lattice to which each atom can be ascribed. So our first goal is to develop a formalism which would allow to map a coherent heteroepitaxial system with continuous variables onto a lattice gas model with only discrete variables. This will be done in Secs. II–IV. The techniques proposed are rather general and in principle can be applied to any coherent system in any number of dimensions. But in order to simplify explanation of basic ideas, in the present paper we restrict ourselves to the simplest case of 1D systems.

Besides their simplicity and convenience for theoretical studies, 1D heteroepitaxial systems are also of great practical value. One of the important goals of the heteroepitaxial studies is the development of techniques of growing 1D quantum wires which can be used, e.g., for experimental investigation of the Luttinger model of interacting 1D electrons.[8] Furthermore, the quantum wires may find application in microelectronics circuitry[3] and in magnetic memory devices.[9] The latter applications would require the 1D structures of finite and equal length. This requirement can be satisfied by self-assembled size calibrated structures similar to quantum dots of the 2D epitaxy.[2]

A phenomenological theory explaining the mechanism of formation of quantum dots was proposed in Ref. 5. The theory is quite general and can be applied to objects in any number of dimensions. So to illustrate the techniques developed in the present paper we will study the conditions of formation of the 1D size calibrated monatomic chains in two heteroepitaxial systems in Sec. III E. Besides, in Sec. IV C a new phenomenon of transient self-assembly at finite temperature will be discussed and the exact cluster size distributions for the model with parameters corresponding to the Pt/Co system will be calculated. In conclusion we will briefly discuss the possibility of experimental verification of the 1D self-assembly.

II. THE MODEL

Let us consider a 1D ''surface'' with a coherent atomic structure deposited on it. Considering the atoms as classical objects we can write the energy of the system as a function of atomic coordinates

$$E_{tot} = U(\{R_i, u_i\}), \tag{1}$$

where R_i are the coordinates of the lattice sites which are filled with atoms and u_i is the displacement of the atom from its ideal position at R_i. The lattice is considered to be periodic, so in 1D case

$$R_i = ai, \tag{2}$$

where a is the lattice constant and i is an integer.

At zero temperature, the state of the system can be exhaustively characterized by its atomic configuration which is described by the set of the occupation numbers $\{n_i^A = 0,1\}$ of the lattice sites $\{R_i\}$, where the superscript A differentiate atoms of different kinds (for example, those of the substrate and of the adlayer). This is because the atomic displacements can be found by minimization of $U(\{R_i, u_i\})$ with respect to $\{u_i\}$. Thus, the total energy (1) can be considered as a function of the variables $\{n_i^A = 0,1\}$ only. In practical calculations this function can be expanded into a series over the complete set of independent polynomials of variables $\{n_i^A = 0,1\}$, as explained in Ref. 10. The lattice gas model thus obtained may be used to study the ground-state structures of the original model (1) with the use of techniques developed for such models (see Ref. 10 for details).

At finite temperature the above technique does not apply because all variables become fluctuating quantities and only their average values can be calculated and/or measured. At low temperatures, however, the atomic dynamics also admits description in terms of variables $\{n_i^A\}$ only because in this case the deviation variables can be integrated out in the course of statistical averaging as follows. The dominant processes of atomic kinetics at surfaces are activated hops over the energy barriers separating lattice sites.[11] Because the probability of the hops is subject to the Arrhenius law, the hop frequency at low temperatures can be arbitrarily small or, equivalently, the residence time can be arbitrarily large. The dynamics of the variables $\{u_i\}$, on the other hand, do not have any energy barriers. So at sufficiently low temperature these variables are capable of reaching their thermal equilibrium distribution during the time intervals between the atomic hops, i.e., with the atomic configuration remaining unchanged. Averaging over u_i will leave us with an effective nonequilibrium free energy function F_{eff} of variables $\{n_i^A\}$ only:

$$\exp(-F_{eff}/k_BT) = C \int \prod_{\{n_i^A = 1\}} du_i \exp(-U/k_BT), \tag{3}$$

where integration is carried over the atomic coordinates of filled sites and C denotes a constant of dimension $[\text{length}]^{-N}$ (N is the number of atoms) to make the integral dimensionless. This purely lattice model can be further used in both equilibrium and kinetic studies.

To illustrate this general approach with an explicitly solvable example we consider a simple 1D model by assuming that the deposited atoms are of the same kind and that the substrate is rigid and does not participate in the dynamics. We will work in the formalism of the canonical ensemble, i.e., by considering the number of atoms N to be constant in all processes. Therefore, we will not be interested in explicit expressions of the quantities which depend only on the total number of atoms—like the constant C in Eq. (3)—because both in kinetic[6] and equilibrium problems only relative weights of configurations are important, so the factors which remain constant under configuration changes cancel out.

A. Pair potential interatomic interaction

The cluster expansion formalism[10] is a universal technique and can be applied to any energy functional of the type of Eq. (1). But in order to illustrate the essence of our approach in the most elementary way we assume simple pair potential interaction between the atoms and write the energy functional as

$$U = \sum_{\text{filled } i} V_s(R_i + u_i) + \frac{1}{2} \sum_{\text{filled } ij} V_p(u_i + R_i - u_j - R_j), \tag{4}$$

where V_s is the potential binding of the deposited atom to the substrate, V_p is the pair potential of interaction between the deposited atoms, and the summations are carried only over the sites filled with adatoms. The pair potential interaction between the adatoms and the atoms belonging to the substrate reduces to the one-body potential $V_s(r)$ when summed over the substrate atoms whose positions are fixed according to our assumption of passive substrate.

The main difficulty in going from the energy functional (4) to the effective free energy F_{eff} consists in the necessity to calculate the multiple integral in Eq. (3) which in the thermodynamic limit is of infinite dimension. To overcome this difficulty we first neglect pair interatomic interaction V_p between the atoms which are not nearest neighbors (NN). In this case the adatoms which are separated by at least one empty site do not interact, so the energy functional (4) takes the form of the sum over contiguous chains of atoms

$$U = \sum_{\text{chains}} \left[\sum_{i=1}^{l} V_s(R_i + u_i) + \sum_{i=1}^{l-1} V_p(a + u_{i+1} - u_i) \right] \equiv \sum_{\text{chains}} U_l, \tag{5}$$

where we used Eq. (2) to simplify the argument of V_p. The first summation on the right-hand side (rhs) is over the atomic chains of various lengths $l, l = 1 - N$. Here and below the summation is supposed to amount to zero if its upper limit is smaller than the lower one, as is the case in the second term of Eq. (5) for $l = 1$.

Correspondingly, the integral in Eq. (3) transforms into the product of integrals as

$$\exp(-F_{\text{eff}}/k_BT) = C \prod_{\text{chains}} \int \left(\prod_{i=1}^{l} du_i \right) \exp[-U_l/k_BT]. \tag{6}$$

Thus, the problem is reduced to the calculation of the multiple integral over the displacement variables belonging to one atomic chain. This question is discussed below in detail.

B. Harmonic approximation and misfit

The multiple integration in Eq. (6) still remains hardly feasible in the case of general $V_s(r)$ and $V_p(r)$. To make the task tractable we further simplify the integrand with the use of the harmonic approximation which is a standard tool in dealing with atomic displacements.[12] Thus, expanding the potentials up to the second order in the displacement variables we get

$$V_s(R_i+u_i)\approx V_{s0}+\frac{k_s}{2}u_i^2,$$

$$V_p(a+u_{i+1}-u_i)\approx V_{NN}+V'(a)(u_{i+1}-u_i)+\frac{k_p}{2}(u_{i+1}-u_i)^2,$$

$$=V_{NN}+\frac{k_p}{2}[(u_{i+1}-u_i-f)^2-f^2], \qquad (7)$$

where $V_{s0}=V_s(R_i=0)$ (and is independent of R_i because of the periodicity) and $V_{NN}=V(a)$ are the zeroth order terms of the expansion. $k_s=V_s''(0)$ and $k_p=V_p''(a)$ are the second derivatives of potentials V_s and V_p, respectively. In the harmonic approximation they play the role of the stiffness constants of the springs binding the atoms to the substrate (k_s) and to each other (k_p). The linear term is absent in the case of V_s because of the left/right symmetry of the substrate potential. In the last line of Eq. (7) we represented the harmonic interatomic interaction in the form familiar from the Frenkel-Kontorova model. The latter is frequently being used in qualitative[13–15] and semiquantitative studies[16,17] of strained epitaxy. The misfit parameter in our case is

$$f=-V_p'(a)/k_p.$$

In our opinion, this definition is quite reasonable from a physical point of view because it defines the misfit through the ratio of the restoring force exerted by an atom on its neighbor ($-V_p'$) to the stiffness of the spring which binds these atoms. Thus, the misfit would correspond to the elongation of the spring under the influence of the force applied.

We note that the ranges of validity of the power-series expansions in Eq. (7) are different for V_s and V_p. In the case of V_s the expansion is in powers of u_i, while in the case of V_p it is in powers of $u_{i+1}-u_i$. So in the second case the deviations themselves can be large but it is the difference of deviations of neighboring atoms which should be small. This observation will be important in assessing the range of validity of the solutions of the equations below.

To check the quality of our approximations of the potential V_p we applied them to the Ag-Ag Morse potential proposed in Ref. 16 for the Ag atoms deposited on Pt substrate. From Fig. 1 one can see that the quality of the fit is satisfactory for $|u_{i+1}-u_i|<f$. In the case of the Ag/Pt system f is positive. The misfit is also positive in the majority of the systems exhibiting self-assembly.[15] Therefore, for simplicity we will assume $f>0$ throughout the present paper.

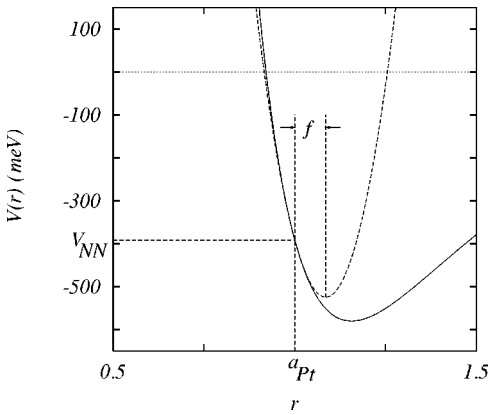

FIG. 1. Morse potential fitted to the interatomic interaction of Ag atoms taken from Ref. 16 (solid line) together with the harmonic fit according to Eq. (7) (dashed parabola). The length unit is the lattice constant of Pt(111) substrate surface: $a_{Pt}=2.77$ Å. V_{NN} is the NN interatomic interaction and f is the misfit parameter as defined in the text.

III. SELF-ASSEMBLY AND SIZE CALIBRATION AT ZERO TEMPERATURE

As we pointed out in the Introduction, one of the most interesting topics in strained epitaxy is the size calibration of self-assembled clusters. In this section we consider the conditions of the size calibration in our 1D model. To begin with, let us assume that our N-atoms system has separated into N/l clusters of length l. In order to be energetically favorable such a configuration should minimize the total energy of the system:

$$\min E_{tot}=\min\left(\frac{N}{l}E_l\right)=N\min(E_l/l), \qquad (8)$$

where E_l is the energy of the l-atom cluster (or chain). In the last equality we made use of the condition $N=\text{const}$. Thus, the system will separate into N/l_{min} clusters provided E_l/l has a minimum at some finite value of $l=l_{min}$. The energy of a chain of length l in the harmonic approximation can be found as the minimum of the functional

$$U_l=\frac{k_s}{2}\sum_{j=1}^{l}u_j^2+\frac{k_p}{2}\sum_{j=1}^{l-1}[(u_{j+1}-u_j-f)^2-f^2]+(l-1)V_{NN}$$
$$=\frac{k_s}{2}\sum_{j=1}^{l}u_j^2+\frac{k_p}{2}\sum_{j=1}^{l-1}(u_{j+1}-u_j)^2+k_pf(u_1-u_l)+(l-1)V_{NN}, \qquad (9)$$

which is obtained as the sum of the expansions, Eq. (7), from every atom and for every pair of atoms entering the chain. The term proportional to V_{s0} is omitted because when summed over all chains it is proportional to N and thus is configuration independent. The last line in Eq. (9) was obtained by expanding the Frenkel-Kontorova term in the square brackets. We see that if the chain fills all the surface and periodic boundary condition $u_1=u_l$ is being used then the chain energy, Eq. (9), does not depend on f. This is be-

cause the linear terms of the expansion drop as the system becomes left-right symmetric, as in the case of V_s. This does not mean, however, that the misfit becomes irrelevant. The strain energy enters implicitly through V_{NN}, as can be seen from Fig. 1. The linear in f terms, however, are responsible for the strain relaxation,as we will see below.

A. The atomic relaxation

To find the chain energy E_l we have to minimize U_l with respect to the atomic displacements u_i:

$$\partial U_l/\partial u_j=0, \quad j=1,\ldots,l \tag{10}$$

or explicitly

$$\begin{aligned}
&(1+\alpha)u_1-u_2=-f,\\
&\vdots\\
&-u_{j-1}+(2+\alpha)u_j-u_{j+1}=0,\\
&\vdots\\
&(1+\alpha)u_l-u_{l-1}=f,
\end{aligned} \tag{11}$$

where we divided both sides of Eq. (10) by k_p to show that the equations (hence, their solutions) depend on the spring constants k_s and k_p only through their dimensionless ratio $\alpha=k_s/k_p$. Because of the cancellation of linear terms in Eq. (9) mentioned above, the equations for $j=2,\ldots,l-1$ (denoted above by dots) are all homogeneous. We note that they are a discrete version of the linear differential equation of the second order

$$-d^2u/dx^2+\alpha u=0.$$

So their solution should be sought in the form of a linear combination of two independent solutions of the form exp $(\pm\lambda j)$. It is straightforward to check that in the discrete case

$$e^{\pm\lambda}=1+\frac{\alpha}{2}\pm\sqrt{\alpha\left(1+\frac{\alpha}{4}\right)}, \tag{12}$$

where the signs were chosen so that λ was positive. The coefficients C_1 and C_2 in the general solution

$$u_j=C_1e^{\lambda j}+C_2e^{-\lambda j} \tag{13}$$

are found by substituting it into the first and the last (inhomogeneous) equations of the set (11):

$$\begin{aligned}
&e^{\lambda}(1+\alpha-e^{\lambda})C_1+e^{-\lambda}(1+\alpha-e^{-\lambda})C_2=-f,\\
&e^{\lambda l}(1+\alpha-e^{-\lambda})C_1+e^{-\lambda l}(1+\alpha-e^{\lambda})C_2=f.
\end{aligned}$$

With two substitutions (one for the upper and for the lower signs)

$$1+\alpha-e^{\mp\lambda}=\pm\sqrt{\alpha}e^{\pm\phi},$$

where

$$e^{\pm\phi}=\sqrt{1+\frac{\alpha}{4}}\pm\frac{\sqrt{\alpha}}{2}$$

the equations can be written in more compact form

$$\begin{aligned}
&e^{\lambda-\phi}C_1-e^{-\lambda+\phi}C_2=f/\sqrt{\alpha},\\
&e^{\lambda l+\phi}C_1-e^{-\lambda l-\phi}C_2=f/\sqrt{\alpha}.
\end{aligned}$$

From these equations the coefficients C_1 and C_2 are easily found by standard means and being substituted into the general solution (13) lead to the following explicit expression for the atomic displacements

$$u_j=-\frac{f}{\sqrt{\alpha}}\frac{\sinh[\lambda(l-2j+1)/2]}{\cosh[\lambda(l-1)/2+\phi]}. \tag{14}$$

The displacements are antisymmetric with respect to the middle of the chain

$$u_{l-j+1}=-u_j \tag{15}$$

as it should be from symmetry considerations. In particular,

$$u_l=-u_1.$$

The displacements u_j monotonously grow towards the chain ends and the larger they are the bigger is the chain length. In the limit of infinite chain the displacements are

$$u_j^{\infty}=-\frac{f}{\sqrt{\alpha}}e^{-\lambda(j-1)-\phi} \tag{16}$$

(where by the superscript ∞ we denoted the chain length) which means that atomic relaxation exponentially dies out in the chain interior and only $\sim 1/\lambda$ external atoms exhibit appreciable deviations from their pseudomorphic positions. The largest deviations exhibit the end atoms

$$u_1^{\infty}=-u_l^{\infty}=-\frac{f}{\sqrt{\alpha}}e^{-\phi}=-f\left(\sqrt{\frac{1}{\alpha}+\frac{1}{4}}-\frac{1}{2}\right). \tag{17}$$

B. Validity checks

The above expressions can be used to establish the range of validity of the solutions obtained in terms of restrictions on the microscopic parameters.

The power-series expansion in $\{u_i\}$ in the first line of Eq. (7) should be consistent with the largest atomic displacement Eq. (17). To verify this we note that the periodic substrate potential in the Frenkel-Kontorova model is conventionally modeled by the cosine function

$$V_s(u)\propto\cos(2\pi u/a).$$

It is straightforward to check that the harmonic approximation of Eq. (7) reproduces the u-dependent part $V_s(u)-V_{s0}$ of the exact potential with the accuracy better then 25% for u as large as $u\simeq a/4$ (half way to the cell boundary). This gives a restriction on the parameters

$$\frac{f}{a}\left(\sqrt{\frac{1}{\alpha}+\frac{1}{4}}-\frac{1}{2}\right)\lesssim\frac{1}{4}.$$

From this inequality it follows that even for the misfit as large as 5%, the value of α can be as small as 1/30.

From Eq. (16) it is easily seen that the relative displacement of neighbor atoms is also the biggest near the chain ends. So we may check the validity of the second-order expansion of V_p in Eq. (7) in the most unfavorable case of the infinite chain using the relative displacement of the first two atoms near its end. From the first equation of Eq. (11) we find

$$u_1-u_2=-(f+\alpha u_1). \tag{18}$$

Applying this equation to the chain of infinite length with the use of Eqs. (16) and (12) we find

$$|u_1^\infty-u_2^\infty|=fe^{-\lambda}<f,$$

which means that our solution is compatible with the harmonic approximation for V_p for all values of the parameter α, including small values. Below we will see that small values of α are favorable for the size calibration, so the validity of the harmonic approximation at small values of this parameter means that our formalism is adequate for the description of the self-assembly phenomena.

C. The relaxation energy

In the chain energy functional Eq. (9) it is natural to separate the terms which depend on the atomic displacements:

$$W_l(\{u_i\})=U_l(\{u_i\})-U_l(\{u_i=0\}). \tag{19}$$

For obvious reasons we will call this part of U_l the relaxation energy. The remainder is just the pair interaction energy $(l-1)V_{NN}$.

Next we want to simplify the expression for W_l [which is just Eq. (9) without the last term] with the use of the summation by parts formula derived in Appendix A. With the use of Eq. (A1) and the symmetry relation $u_l=-u_1$, the expression for the relaxation energy Eq. (19) reduces to

$$W_l=k_su_1^2+\frac{k_p}{2}(u_1-u_2)^2+2k_pfu_1+\frac{k_p}{2}(u_1^2-u_2^2),$$

where the first three terms come from Eq. (9) and the last term is from Eq. (A1). This equality can be further simplified with the use of Eq. (18) multiplied by k_p

$$k_p(u_1-u_2)=-(k_pf+k_su_1).$$

With its help the above expression for W_l after a little algebra takes a particularly simple form

$$W_l=k_pfu_1=-V_p'(a)u_1\approx V_p(a-u_1)-V_p(a), \tag{20}$$

which means that the relaxation energy is approximately equal to the pair interaction energy gained by the end atom due to relaxation. According to Eq. (14)

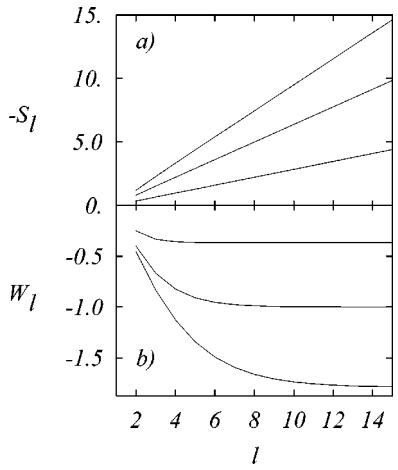

FIG. 2. Relaxation entropy in units of k_B (a) and relaxation energy in units of k_pf^2 (b) for chains of length l. At both figures the first curve from the horizontal zero axis corresponds to $\alpha=2$, the second to $\alpha=0.5$, and the third one to $\alpha=0.2$ (note difference in scale).

$$u_1=-\frac{f}{\sqrt{\alpha}}\frac{\sinh[\lambda(l-1)/2]}{\cosh[\lambda(l-1)/2+\phi]}.$$

In Fig. 2(b) the relaxation energy is plotted for three values of the parameter α. As follows from Eq. (20) these curves are also (up to a constant factor) the plots of the dependence of the chain elongation on the chain length.

D. Size calibration criteria

According to Eq. (8) and Ref. 5, the size calibration takes place in the case when the function E_l/l has a minimum at some finite value of l. This can be used to express the conditions of the size calibration in terms of the model parameters. To this end we first observe that if some function of l has a minimum at some finite value of $l=l_{min}$ then for $l>l_{min}$ this function is growing as $l\to\infty$. Let us consider the large-l behavior of the reduced chain energy

$$E_l=W_l+(l-1)V_{NN} \tag{21}$$

at zero temperature

$$\frac{E_l}{l}=\frac{W_l+(l-1)V_{NN}}{l}\approx_{l\to\infty}V_{NN}+\frac{W_\infty-V_{NN}}{l}. \tag{22}$$

Because the approach of W_l to its $l\to\infty$ limiting value is exponentially quick, the asymptotic behavior is dominated by the slow $1/l$ dependence, so we replaced the relaxation energy by W_∞. Thus, the reduced energy in Eq. (22) is a growing function of l at large values of chain lengths if the following inequality holds,

$$W_\infty-V_{NN}<0.$$

Assuming that V_{NN} is negative and taking into account that W_∞ is also negative [see, e.g., Fig. 2(b)], it is convenient to rewrite the above inequality in terms of the absolute values

TABLE I. Parameters corresponding to the Pt/Co heteroepitaxial system.

ϵ	f/a_{Co}	α	$k_p f^2$ (eV)	V_{NN} (eV)
0%	3.5%	0.32	0.049	−0.218
2%	4.4%	0.25	0.100	−0.179
3%	4.8%	0.22	0.136	−0.152

$$|V_{NN}|<|W_\infty|. \tag{23}$$

The meaning of this condition is simple. The left-hand side (lhs) is the loss in the binding energy because of the separation of a long chain into two pieces. The rhs is the energy gain due to the relaxation of the two free ends that appear. Thus, if the gain is larger than the loss the chain is unstable with respect to decomposition into smaller parts. The process of decomposition will end when all pieces acquire the optimum length l_{min}.

Substituting the explicit expression for W_∞ from Eqs. (20) and (16) into Eq. (23), one can express the calibration criterion in terms of the microscopic parameters as

$$k_p f^2\left(\sqrt{\frac{1}{\alpha}+\frac{1}{4}}-\frac{1}{2}\right)>|V_{NN}|. \tag{24}$$

From this inequality we see that the self-assembly into size-calibrated clusters requires that the binding of atoms through V_{NN} was not too strong. Also, the stiffness of the spring binding of the atom to the substrate should be small compared to k_p (i.e., $\alpha=k_s/k_p$ should be small). Large misfit and the stiffness k_p of the interatomic ''spring'' are also favorable for the clustering. From Fig. 1 one can see that with our definition of $f=-V_p'/V_p''$ the misfit would have been zero for the substrate lattice constant a near the minimum of V_p. $|V_{NN}|$ in this case would have had the largest value, so the inequality (24) would have been strongly violated. With diminution of a all the conditions favorable for the self-assembly start to improve: $|V_{NN}|$ diminishes, f and k_p grow because of the growing steepness of the $V_p(r)$ curve, and even α is most probably diminishing because in its definition k_p is in the denominator while on physical grounds one may expect that k_s depends weakly on a because in the cell center atomic potentials are much less steep than in the near-core region. This is confirmed by calculations of the next section (see the third column of Table I). Thus, we conclude that by compressing the substrate one can considerably improve the conditions for the self-assembly of size calibration clusters. This will be illustrated with concrete calculations in the following section.

E. Examples from metallic heteroepitaxial systems

To illustrate the above formalism with realistic examples of strained epitaxy we consider two metallic heteroepitaxial systems—Ag/Pt and Pt/Co—which currently are being actively studied both experimentally[18–20] and theoretically.[21–23] For simplicity we consider 1D case and use the geometry of Ref. 23, where the growth on the steps of the close-packed vicinal surfaces was studied. The position of a deposited atom was relaxed to its equilibrium value in order to find the value k_s as the second derivative of the potential near equilibrium. The many-body ''potentials'' and corresponding parameters were taken from Ref. 23 for the Ag/Pt system and from Ref. 22 for the Pt/Co system. These potentials were devised specifically for application in the heteroepitaxy and for the close-packed surfaces [(111) in the Ag/Pt case and (0001) in the Pt/Co system] so we expect our results below are quite reliable. Although interatomic interactions in Refs. 21–23 do not have the pair potential form (4) but include nonlinear many-body corrections due to the band-structure effects, we hope that the few parameters entering our solution can be reliably calculated with the use of this formalism. In this respect our approach is similar to Ref. 17 where the parameters of the Frenkel-Kontorova model were fitted directly to the band-structure calculations.

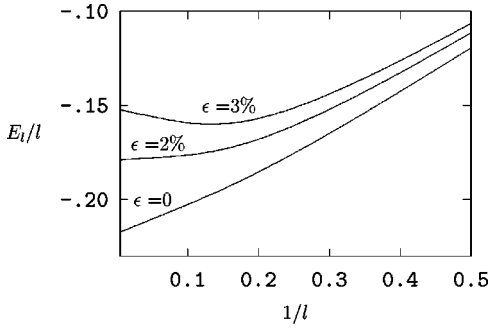

FIG. 3. Length dependence of the reduced energy at zero temperature of the Pt monatomic chains for different values of compression ϵ of the Co substrate.

The parameters listed in Table I were calculated for the atomic pairs relaxed only in vertical position because in our approach we need the first and second derivatives [see discussion after Eq. (7)] calculated for the pseudomorphic positions of the deposited atoms.

According to our calculations, the Ag/Pt system has the following parameters[23] (the energy unit is eV and the length unit Å): $V_{NN}^p\approx-0.57$, $V_{NNN}^p\approx-8.8\times10^{-3}$, $k_pf^2\approx0.72$, and $\alpha\approx3.7$. Here V_{NNN}^p is the next NN (NNN) interatomic interaction. Its smallness in comparison with V_{NN}^p justifies our NN approximation. The large value of α means that the relaxation of the strain is very weak (see Fig. 2) so there is no size calibration with the above parameters. The crucial parameter α, however, can strongly vary in different systems. For example, according to our estimates based on the potentials of Ref. 22, in Pt/Co this parameter is an order of magnitude smaller, $\alpha\simeq0.32$. Because of this the system is quite close to the self-assembly but the misfit strain is still too small. To enhance the misfit in our model calculations we assumed that the Co underlayer is further compressed (e.g., by means of deposition on an appropriate substrate) by the factor $1-\epsilon$. (see Table I and Fig. 3). From the figure it is seen that for $\epsilon=3\%$ the curve E_l/l does have a minimum in which case the qualitative analysis of Ref. 5 applies. The exact solution of Ref. 24 confirms the major qualitative conclusion of the above paper about the size calibration at lowering temperature. Besides, it was shown that in the presence

of a NNN attraction the clusters will self-organize into regular arrays. This phenomenon may be of importance in the technological applications mentioned in the Introduction.

IV. EXACT SOLUTION AT FINITE TEMPERATURE

In this section we will consider a finite temperature solution of the harmonic Frenkel-Kontorova model which we defined in Sec. II and solved at zero temperature in Sec. III. To this end we first integrate out the continuous displacement variables (following section). In Sec. IV B the model is solved exactly at thermal equilibrium. In Sec. IV C, this solution is used to predict a new phenomenon of transient self-assembly which cannot be predicted neither from the zero-temperature solution of the preceding section, nor from the finite-temperature theory of Ref. 5. Finally, in Sec. IV D we conclude our present study by mapping the system onto a lattice-gas Hamiltonian which can be used in dealing with 2D systems and/or in kinetic Monte Carlo simulations.

A. Averaging over atomic displacements

As was pointed out in Sec. II, at finite temperature the lattice-gas model can be obtained by means of statistical averaging over the displacement variables with atomic configuration $\{n_i^A\}$ being kept fixed. The harmonic approximation in this case makes it possible to perform the multiple integration in Eq. (6) with the use of the known formula for multidimensional Gaussian integral which is presented in Appendix B. To apply formulas derived the Appendix to the multiple integral in Eq. (6) we first set $M=D_l/k_BT$, where D_l is the dynamical matrix corresponding to the quadratic in $\{u_i\}$ form in Eqs. (9) or (19):

$$D_l=\begin{pmatrix} k_p+k_s & -k_p & 0 & \dots & 0 & 0 & 0 \\ -k_p & 2k_p+k_s & -k_p & 0 & \dots & 0 & 0 \\ 0 & -k_p & 2k_p+k_s & -k_p & 0 & \dots & 0 \\ \vdots & \vdots & \ddots & \ddots & \ddots & \vdots & \vdots \\ 0 & \dots & 0 & -k_p & 2k_p+k_s & -k_p & 0 \\ 0 & 0 & \dots & 0 & -k_p & 2k_p+k_s & -k_p \\ 0 & 0 & 0 & \dots & 0 & -k_p & k_p+k_s \end{pmatrix}_{l}. \tag{25}$$

In Appendix B we have shown that the exponent of the Gaussian integral Eq. (B1) is equal to the minimum of the exponent of the integrand, so we can immediately write

$$\int \left(\prod_{i=1}^{l} du_i\right) \exp\left(-\frac{U_l}{k_BT}\right) = \exp\left[-\frac{1}{2}\ln\left(\det\frac{D_l}{2\pi k_BT}\right)-\frac{E_l}{k_BT}\right] \tag{26}$$

because the minimum of the quadratic form in U_l was already calculated in Sec. III C to be equal to W_l and E_l appears because of Eq. (21). Further, because the determinant of a matrix is a homogeneous function of the matrix elements of the order of the matrix size (which is l in our case), the constant multipliers of the matrix under the determinant sign in Eq. (26) can be separated out into a term of the type $l\ln(2\pi k_BT/c)/2$ with some arbitrary constant c. When summed over all chains these factors will accumulate the configuration independent factor N and so may be dropped as long as we are interested only in configuration dependent quantities. It is convenient to choose this constant to be equal to $D_1=k_s$, the dynamical matrix of an isolated atom because with this choice the logarithmic term vanishes when the atomic displacements became unrestricted. This would correspond to $k_p=0$ in which case the dynamical matrix (25) would be proportional to the unit matrix: $D_l=k_sI$ and when divided by $D_1=k_s$ would have its determinant equal to unity. By analogy with Eq. (3) we will write the exponential function on the rhs of Eq. (26) as $\exp(-F_l/k_BT)\equiv\exp(S_l/k_B-E_l/k_BT)$ with the entropy due to the atomic displacements

$$S_l=-\frac{k_B}{2}\ln\det\left(\frac{\overline{D}_l}{\overline{D}_1}\right), \tag{27}$$

where we additionally divided the numerator and denominator under the sign of the determinant by k_p to make the matrices dimensionless:

$$\overline{D}_l=D_l/k_p, \quad \overline{D}_1=k_s/k_p=\alpha.$$

The term *entropy* was used because due to temperature independence of both E_l and S_l we have $S_l=-\partial F_l/\partial T$, which is an expression for the entropy in the canonical ensemble. We note that this quantity is, in fact, only a part of the total entropy due to displacements because we neglected the contribution proportional to N.

Explicit expression for the chain entropy can be obtained by exploiting the tridiagonality of the dynamical matrix (25). Such matrices satisfy the recurrence relations presented in Appendix C. Because $\bar{D}_1=\alpha$, the chain entropy Eq. (27) with the use of Eq. (C8) takes the form

$$S_l=-\frac{k_B}{2}\left[\ln\left(\sqrt{\frac{\alpha}{1+\alpha/4}}\sinh[\lambda(l-1/2)+\phi]\right)-l\ln\alpha\right]. \tag{28}$$

S_l calculated with this formula is shown in Fig. 2(a). The entropic contribution is negative because in our formalism we discarded the entropy term corresponding to $k_p=0$, as explained above. When k_p is not equal to zero, the atomic displacements became restricted by its neighbors, so their entropy diminishes. For large chains the interior atoms are practically in translationally invariant environment, so for long chains the entropy loss is proportional to l. The above restrictions on the atomic displacements are more stringent for larger k_p. This is reflected in the slope of S_l which is larger for smaller $\alpha=k_s/k_p$ [see Fig. 2(a)].

B. Configurational averaging

Thus, for an individual chain we completely disposed of the continuous variables $\{u_i\}$ both at zero and at finite temperature. Our results can be summarized in the expression for the effective free energy of the chain of length l as

$$F_l=E_l-TS_l, \tag{29}$$

where E_l and S_l are given by Eqs. (21) and (28), respectively. Thus, Eq. (6) takes the form

$$\exp(-F_{\text{eff}}/k_BT)=C\exp\left(-\sum_{\text{chains}}F_l/k_BT\right). \tag{30}$$

Here in constant C we gathered all configuration independent factors which are irrelevant for the current study.

The partition function of the system under consideration can be found by summing Eq. (30) over all possible atomic configurations. We note that the weight factor in Eq. (30) looks formally as the canonical Boltzmann weight except that instead of the energy of the chain configuration we have the sum of F_l. This means that in the canonical expression for the equilibrium free energy

$$F_{eq}=E-TS, \tag{31}$$

we should interpret E as the sum of F_l with appropriate weights. Physically this can be understood as follows. In the configurations consisting of chains of different length the chains itself can be considered as linear molecules with their own internal structure which includes, in particular, the internal atomic displacements which are not influenced by their permutations and different placements on the substrate as long as these chains remain separated. In the case when two or more chains become nearest neighbors they are treated as a new ''molecule'' of longer length, the internal free energy of which should be computed according to Eq. (29). Thus,

$$E=\sum_l m_lF_l,$$

where m_l is the number of chains of length l. To compute the entropy S in Eq. (31) we have to count all possible configurations corresponding to a fixed chain length distribution $\{m_l\}$. The number of inequivalent permutations of the chains are

$$\Omega_{chains}=\frac{m_{tot}!}{m_1!m_2!\ldots m_N}, \tag{32}$$

where $m_{tot}=\Sigma_{l=1}^{N}m_l$. Besides the permutations, the chains with a fixed relative order can be differently spaced.[26] So Ω_{chains} should be multiplied by the number of different possible placements of a given chain sequence on the substrate. We will denote this factor by Ω_v. Assuming that the substrate consists of K deposition sites, we use the property of the 1D system that the number of contiguous intervals of vacant sites separating the atomic chains is equal to m_{tot} with a possible difference in ±1 interval due to the substrate boundaries. We neglect this difference in the thermodynamic limit and calculate Ω_{chains} as the number of ways to divide $K-N$ vacant sites into m_{tot} clusters. This is equal to the number of ways to chose $m_{tot}-1$ cuts out of $K-N-1$ possibilities. The latter quantity is given by the binomial coefficient[26]

$$\Omega_v=\binom{K-N-1}{m_{tot}-1}\simeq\frac{(K-N)!}{m_{tot}!(K-N-m_{tot})!}.$$

So the entropy per site $s=S/K=k_B\ln(\Omega_{chains}\Omega_v)$. Assuming $K\to\infty$, with the use of Eq. (32) and the Stirling formula the entropy density is calculated as

$$s=k_B\Big[(1-\theta)\ln(1-\theta)-(1-\theta-c)\times\ln(1-\theta-c)-\sum_l c_l\ln c_l\Big],$$

where $\theta=N/K$ is the total coverage, $c_l=m_l/K$ is the concentration of clusters of length l, and $c=\Sigma_l c_l$ is the total cluster concentration. The concentrations c_l should minimize the functional

$$\omega=\sum_l c_lF_l-k_BTs-\mu\left(\sum_l lc_l-\theta\right),$$

which consists of the free-energy density F_{eq}/K [cf. Eq. (31)] and the constraint $N=\text{const}$ expressed in terms of cluster variables multiplied by the Lagrange multiplier μ. From the minimality condition $\delta\omega/\delta c_l=0$, we obtain an expression for the equilibrium cluster concentrations

$$c_l=(1-\theta-c)\exp[(\mu l-F_l)/k_BT]. \tag{33}$$

This expression with μ adjusted to satisfy the requirement $\Sigma_l lc_l=\theta$ gives the exact equilibrium distribution of cluster lengths in our 1D model. Qualitative behavior of the solutions of Eq. (33) in the case when the size calibration criteria

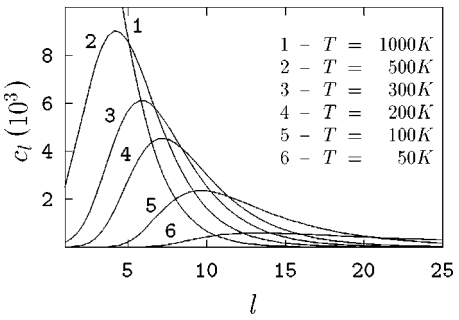

FIG. 4. Model calculation of the transient self-assembly of Pt chains at the steps of the 2% compressed Co substrate at the coverage $\theta=0.3$, c_l is the concentration of chains of length l. The points are connected by splines for better readability (for further details see the text).

are fulfilled is discussed in detail in Ref. 24. In the followng section we consider a solution of this equation in the case when the parameters of the system do not exhibit the size calibration behavior at $T=0$ but the system is close to this regime.

C. Transient self-assembly

In the Pt/Co system considered in Sec. III E, for ϵ below the critical value $\epsilon_c \approx 2\%$, there is no self-assembly at $T=0$ because there is no minimum at finite l in E_l/l (see Fig. 3). This means that the interatomic attraction is too strong. However, because the entropic contribution S_l [see Fig. 2(a)] is practically linear in l, it can be unified with the pair interaction term $(l-1)V_{NN}$ and thus can be considered as a temperature-dependent *repulsive* contribution into the pair interaction. At physically acceptable temperatures it will not be too large in comparison with V_{NN} because in temperature units $V_{NN} \gtrsim 4000$ K (see Fig. 1) while experimental temperatures are usually considerably smaller. Nevertheless, for ϵ slightly below ϵ_c the curve $F_l(T)/l$ will have a T-dependent minimum at some reasonably high temperatures because of the entropic contribution which will disappear at some smaller temperature.

In Ref. 24 it was shown that at nonzero temperature the position of the maximum of the cluster size distribution does not coincide with the minimum of the $F_l(T)/l$ curve, so the position and even the very existence of the size calibration can be seen only from the solution of the statistical problem at the temperature of interest.

In Fig. 4 the size distribution of self-assembled clusters calculated with the use of Eq. (33) is shown. From this figure one can see that our model predicts a new phenomenon: the entropy driven transient self-assembly. It has two salient features which differ from known phenomena. First, the behavior seen in Fig. 4—the appearance and diminution of self-assembled clusters at growing temperature—is opposite to what is usually seen in the kinetically controlled growth.[28] Second, in contrast to the nontransient self-assembly, the width of the size distribution is broadening at lowering temperature. Because this behavior is explained by the relatively weak entropic contribution into the pair interaction energy, observation of such a behavior means that the system is close to the size calibration at $T=0$.

D. Mapping onto lattice-gas models

In an out of equilibrium system or in higher dimensions exact solutions are difficult to obtain, so approximate or numerical techniques should be used. To apply such techniques one would like to have the Hamiltonian of the system under study to be expressed in terms of familiar occupation numbers $\{n_i\}$. With the chain free energy F_l being known for all chain lengths, exact form of the Hamiltonian in 1D can be easily constructed as follows.[24] Taking into account the fact that the chains separated by at least one empty site are not interacting, we assume the Hamiltonian to consist exclusively of the products of the occupation numbers within contiguous atomic chains

$$H=\sum_{i;l\geq 2} v_l n_i n_{i+1}\cdots n_{i+(l-1)}. \tag{34}$$

The parameters v_l can be found from the free energies F_l as follows. If an atom is added to a chain of length l, the free energy of the new chain according to Eq. (34) is

$$F_l=F_{l-1}+v_l+v_{l-1}+v_{l-2}+\cdots+v_2.$$

Writing down similar equation for the chain of length $l-1$ and comparing it with the above equation one easily finds[24]

$$v_l=F_l-2F_{l-1}+F_{l-2}, \tag{35}$$

which is valid for all $l\geq 1$ if we formally set $F_0=F_{-1}=0$. This expresses parameters v_l through the discrete second derivative of F_l. Because the latter according to Eqs. (21) and (28) is asymptotically linear to l, the approach to asymptotics being exponential, the Hamiltonian parameters v_l are exponentially small for large l. This makes possible to restrict the sum over l in Eq. (34) to a desirable level of accuracy. In particular, the entropic term (28) essentially contributes only into the pair interaction v_2, the multiatom contributions being $\lesssim 10\%$. This confirms the qualitative conclusion made in previous section that the relaxation entropy formally amounts to effective NN interatomic repulsion which grows linearly with temperature. The entropic forces of this kind were earlier discovered in alloys (see Appendix E of Ref. 25 and references to earlier literature therein).

In two dimensions and with a rectangular geometry atomic relaxations along two orthogonal directions are independent,[13,14] so Eq. (34) can be straightforwardly generalized to 2D case. In the anisotropic case the parameters v_l can be different along two orthogonal directions but their expression through the microscopic parameters in both cases are the same. In Ref. 27, we applied Monte Carlo technique to a simple isotropic 2D Hamiltonian of the above type to illustrate the size calibration of self-assembled square ''plaquettes'' of the type predicted in Ref. 5.

V. CONCLUSION

In this paper we considered a simple model of strained 1D epitaxy and have rigorously shown that the mechanism of self-assembly and size calibration proposed in Ref. 5 is essentially correct at least for the submonolayer growth. While the simplicity of the model makes its quantitative predictions to be of limited accuracy, we believe that the qualitative picture of the self-assembly of size calibrated clusters is captured by this model correctly. An additional advantage of the model is that all calculations can be performed analytically, so all pertinent questions can be answered in a rigorous and unambiguous manner.

As we noted in the Introduction, despite its simplicity, the Frenkel-Kontorova model has been successfully used in semi-quantitative analyses of ground-state properties of real systems (see, e.g., Refs. 17 and 16). So it may be hoped that the finite temperature generalization of the model given in the present paper can be used to make semiquantitative predictions of some temperature-dependent phenomena concerning *coherent* structures, such as the self-assembly.

We considered two explicit examples of heteroepitaxial systems for which there exist in literature reliable interatomic potentials adjusted to treat heteroepitaxial problems of the type considered by us.[21–23] With these potential we found the size calibration for stressed substrate in Pt/Co system. In our opinion, this shows that the above phenomena should be as common in 1D as they are in 2D heteroepitaxy. Further argument in favor of this conclusion is that for the size calibration to be plausible, the crucial parameter $\alpha = k_s/k_p$ should be as small as possible. This favors small values of k_s. The geometry of Ref. 23 considered by us is not quite favorable because of the high coordination of the atoms deposited at the steps of the vicinal surfaces. The deposited atoms interact with five NN of the substrate (see Ref. 23) which enhances k_s. It may be hoped that with lower coordination (as in the case of 1D structures of Ref. 8), the conditions for the size calibration will be more favorable. Furthermore, the metal/metal systems with strong mutual binding considered in this paper are not very suitable for the search of the size calibration. It seems that the heteroepitaxial pairs with differing types of bonding are more plausible candidates. In our opinion, more promising in this respect are metal/oxide systems where the binding of the metal atoms to the substrate were found to be particularly weak.[29]

ACKNOWLEDGMENTS

One of the authors V.T. expresses his gratitude to University Louis Pasteur de Strasbourg and IPCMS for their hospitality and CNRS-NAS of Ukraine exchange program for financial support.

APPENDIX A

The summation by parts formula which we need to simplify the expression for the relaxation energy is derived as follows. First we introduce the finite difference operator $\Delta v_j \equiv v_{j+1} - v_j$ and apply it to the product $v_j u_j$:

$$\Delta(v_j u_j) = v_{j+1}\Delta u_j + u_j \Delta v_j .$$

By summing up this identity from $j=2$ to $l-1$ we get

$$\sum_{j=2}^{l-1} \Delta(v_j u_j) = v_l u_l - v_2 u_2 = \sum_{j=2}^{l-1} (v_{j+1}\Delta u_j + u_j \Delta v_j).$$

By identifying u_i with the atomic displacements and assuming $v_{j+1} = \Delta u_j$ one can rearrange the above identity as

$$\sum_{j=2}^{l-1} (u_{j+1} - u_j)^2 = -\sum_{j=2}^{l-1} u_j (u_{j+1} - 2u_j + u_{j-1}) + u_l^2 - u_2^2 ,$$

where due to the antisymmetry of the displacements [see Eq. (15)] $u_l u_{l-1} = u_2 u_1$. Now adding to both sides of the latter equality the term $\alpha \Sigma_{j=2}^{l-1} u_j^2$ we note that the summation on the rhs amounts to zero because of the homogeneous part of Eq. (11). Multiplying the resulting equality by $k_p/2$ and recalling that $\alpha = k_s/k_p$ we finally get

$$\frac{k_s}{2} \sum_{j=2}^{l-1} u_j^2 + \frac{k_p}{2} \sum_{j=2}^{l-1} (u_{j+1} - u_j)^2 = \frac{k_p}{2}(u_l^2 - u_2^2). \quad \text{(A1)}$$

APPENDIX B

The multidimensional Gaussian integral is calculated with the known formula as

$$\int \left(\prod_{i=1}^{l} du_i \right) \exp\left(-\frac{1}{2} \sum_{i,j=1}^{l} u_i M_{ij} u_j + \sum_{i=1}^{l} u_i v_i \right) = \left(\det \frac{M}{2\pi} \right)^{-1/2} \exp\left(\frac{1}{2} \sum_{i,j=1}^{l} v_i M_{ij}^{-1} v_j \right), \quad \text{(B1)}$$

where M is a positive-definite symmetric matrix and v—an arbitrary constant vector. The exponent on the rhs is obtained by completing the square on the lhs as

$$\begin{aligned} E(\{u_i\}) &\equiv -\frac{1}{2} \sum_{i,j=1}^{l} u_i M_{ij} u_j + \sum_{i=1}^{l} u_i v_i \\ &= -\frac{1}{2} \sum_{i,j=1}^{l} (u_i - M_{ij}^{-1} v_j) M_{ij} (u_j - M_{jk}^{-1} v_k) \\ &\quad + \frac{1}{2} \sum_{i,j=1}^{l} v_i M_{ij}^{-1} v_j . \end{aligned} \quad \text{(B2)}$$

The preexponential factor in Eq. (B1) with the change of variables $u_i \to u_i - M_{ij}^{-1} v_j$ reduces to the multidimensional integral

$$\int \left(\prod_{i=1}^{l} du_i \right) \exp\left(-\frac{1}{2} \sum_{i,j=1}^{l} u_i M_{ij} u_j \right). \quad \text{(B3)}$$

It is calculated by means of diagonalization of matrix M with the use of an orthogonal transformation the Jacobian of

which is equal to unity. Eq. (B3) then reduces to the product of the textbook Gaussian integrals

$$\int_{-\infty}^{\infty} dx \exp\left(-\frac{a_i x^2}{2}\right) = \sqrt{\frac{2\pi}{a_i}}.$$

The constants a_i in the above product of integrals are the eigenvalues of matrix M and their product is equal to the determinant in Eq. (B1).

A remarkable property of the Gaussian integration which is important for our study is that the argument of the exponential function on the rhs is equal to the minimal value of the lhs exponent. Indeed, by setting partial derivatives with respect to $\{u_i\}$ of the lhs exponent $E(\{u_i\})$ in Eq. (B2) to be equal to zero one arrives at the matrix equation

$$Mu = v,$$

whose solution is $u = M^{-1}v$. Substituting this into the lhs exponent one gets

$$-\frac{1}{2}\sum_{i,j,k,l}(M^{-1}_{ik}v_k)M_{ij}(M^{-1}_{jl}v_l)+\sum_{ik}(M^{-1}_{ik}v_k)v_i = \frac{1}{2}\sum_{i,j} v_i M^{-1}_{ij} v_j,$$

i.e., the rhs exponent.

APPENDIX C

According to Eq. (25) and the definition of $\bar{D}_l = D_l/k_p$

$$\bar{D}_l = \begin{pmatrix} 1+\alpha & -1 & 0 & \cdots & 0 & 0 & 0 \\ -1 & 2+\alpha & -1 & 0 & \cdots & 0 & 0 \\ 0 & -1 & 2+\alpha & -1 & 0 & \cdots & 0 \\ \vdots & \vdots & \ddots & \ddots & \ddots & \vdots & \vdots \\ 0 & \cdots & 0 & -1 & 2+\alpha & -1 & 0 \\ 0 & 0 & \cdots & 0 & -1 & 2+\alpha & -1 \\ \underbrace{0 \quad 0 \quad 0 \quad \cdots \quad 0 \quad -1 \quad 1+\alpha}_{l} & & & & & & \end{pmatrix},$$

where $\alpha = k_s/k_p$. Because matrices $\bar{D}_l$ are tridiagonal, their determinants satisfy recurrence relations which can be used to calculate them. Expanding $\det \bar{D}_l$ with respect to the first row we get

$$\det \bar{D}_l = (1+\alpha)d_{l-1} - d_{l-2}. \tag{C1}$$

where d_{l-1} is the determinant of the matrix obtained from $\bar{D}_l$ by crossing out its first row and the first column:

$$d_{l-1} = \begin{vmatrix} 2+\alpha & -1 & 0 & \cdots & 0 & 0 \\ -1 & 2+\alpha & -1 & 0 & \cdots & 0 \\ 0 & -1 & 2+\alpha & -1 & 0 & 0 \\ \vdots & \vdots & \ddots & \ddots & \ddots & \vdots \\ 0 & \cdots & 0 & -1 & 2+\alpha & -1 \\ \underbrace{0 \quad 0 \quad \cdots \quad 0 \quad -1 \quad 1+\alpha}_{l-1} & & & & & \end{vmatrix} \tag{C2}$$

and $d_{l-2}, d_{l-3}, \ldots$ are obtained from the previous determinant in the same way. Now, expanding determinant Eq. (C2) with respect to the elements of the first row we get the following three term recurrence relation

$$d_{l-1} = (2+\alpha)d_{l-2} - d_{l-3}, \tag{C3}$$

which is valid for all smaller values of the lower index l except $l=1$ and 2. Recurrence relation Eq. (C3) initialized by two first determinants following from Eq. (C2)

$$d_1 = 1+\alpha$$

and

$$d_2 = 1+3\alpha+\alpha^2 \tag{C4}$$

can be used to calculate all d_i and $\det \bar{D}_l$ through Eq. (C1). With the use of Eq. (C3) expression (C1) for $\det \bar{D}_l$ can be somewhat simplified as

$$\det \bar{D}_l = d_l - d_{l-1}, \tag{C5}$$

where determinants d_i for $i>2$ satisfy homogeneous equation

$$d_{i+1} - (2+\alpha)d_i + d_{i+1} = 0$$

[see Eq. (C3)]. This equation coincides with the homogeneous equation in Eq. (11) and so its general solution should be sought in the same form as the solution for u_j Eq. (13)

$$d_i = c_1 e^{\lambda i} + c_2 e^{-\lambda i} \tag{C6}$$

but with different boundary conditions

$$e^{\lambda}c_1 + e^{-\lambda}c_2 = 1+\alpha,$$

$$e^{2\lambda}c_1 + e^{-2\lambda}c_2 = 1+3\alpha+\alpha^2, \tag{C7}$$

which are obtained by equating general solution (C6) to

known determinants d_1 and d_2 [see Eq. (C4)]. Solving Eq. (C7) from Eq. (C6) we get

$$d_i = \frac{\cosh(\lambda i + \phi)}{\sqrt{1+\alpha/4}}.$$

Substituting this into Eq. (C5) we obtain an analytic expression for the determinant of the dynamical matrix

$$\det \bar{D}_l = \sqrt{\frac{\alpha}{1+\alpha/4}} \sinh[\lambda(l-1/2)+\phi]. \qquad \text{(C8)}$$

[1] D.J. Eaglesham and M. Cerullo, Phys. Rev. Lett. **64**, 1943 (1990); Y.-W. Mo, D.E. Savage, B.S. Swartzentruber, and M.G. Lagally, *ibid.* **65**, 1020 (1990); S. Guha, A. Madhukar, and K.C. Rajkumar, Appl. Phys. Lett. **57**, 2110 (1990).

[2] R. Notzel, J. Temmyo, and T. Tamamura, Nature (London) **369**, 131 (1994); D. Leonard *et al.*, Appl. Phys. Lett. **63**, 3203 (1993).

[3] A.O. Orlov, I. Amlani, C.S. Lent, and G.L. Snider, Science **277**, 928 (1997).

[4] J.H. van der Merwe, D.L. Tönsing, and P.M. Stoop, Surf. Sci. **312**, 387 (1994); M. Henzler, *ibid.* **357–358**, 809 (1996); S. Tan, A. Ghazali, and J.C.S. Lévy, *ibid.* **369**, 360 (1996).

[5] C. Priester and M. Lannoo, Phys. Rev. Lett. **75**, 93 (1995).

[6] K. Binder, in *Monte Carlo Methods in Statistical Physics*, edited by K. Binder, Topics in Current Physics Vol. 7 (Springer-Verlag, Heidelberg, 1986), 2nd ed.

[7] K.E. Khor and S. Das Sarma, Phys. Rev. B **62**, 16 657 (2000).

[8] P. Segovia, D. Purdie, M. Hensenberger, and Y. Baer, Nature (London) **402**, 504 (1999).

[9] J. Dorantes-Dávila and G.M. Pastor, Phys. Rev. Lett. **81**, 208 (1998).

[10] F. Ducastelle, *Order and Phase Stability in Alloys* (North-Holland, Amsterdam, 1991).

[11] C. Uebing and R. Homer, J. Chem. Phys. **95**, 7626 (1991).

[12] A.G. Khachaturyan, *Theory of Structural Transformations in Solids* (Wiley, New York, 1983).

[13] J.A. Snyman and J.H. van der Merwe, Surf. Sci. **45**, 619 (1974).

[14] C. Ratsch and A. Zangwill, Surf. Sci. **293**, 123 (1993).

[15] E. Korutcheva, A.M. Turiel, and I. Markov, Phys. Rev. B **61**, 16 890 (2000).

[16] J.C. Hamilton, R. Stumpf, K. Bromann, M. Giovannini, K. Kern, and H. Brune, Phys. Rev. Lett. **82**, 4488 (1999).

[17] S.C. Erwin, A.A. Baski, L.J. Whitman, and R.E. Rudd, Phys. Rev. Lett. **83**, 1818 (1999).

[18] A.F. Becker, G. Rosenfeld, B. Poelsema, and G. Comsa, Phys. Rev. Lett. **70**, 477 (1993).

[19] P. Gambardella, M. Blanc, H. Brune, K. Kuhnke, and K. Kern, Phys. Rev. B **61**, 2254 (2000).

[20] P. Gambardella, M. Blanc, L. Bürgi, K. Kuhnke, and K. Kern, Surf. Sci. **449**, 93 (2000).

[21] C. Goyhenex and G. Tréglia, Surf. Sci. **446**, 272 (2000).

[22] C. Goyhenex, H. Bulou, J.-P. Deville, and G. Tréglia, Phys. Rev. B **60**, 2781 (1999).

[23] F. Picaud, C. Ramseyer, C. Girardet, and P. Jensen, Phys. Rev. B **61**, 16 154 (2000).

[24] V.I. Tokar and H. Dreyssé, Phys. Rev. E **68**, 011601 (2003).

[25] A. van de Walle and G. Ceder, Rev. Mod. Phys. **74**, 11 (2002).

[26] J. Vavro, Phys. Rev. E **63**, 057104 (2001).

[27] V.I. Tokar and H. Dreyssé, Mol. Phys. **29**, 193 (2002).

[28] H. Röder, E. Hahn, H. Brune, J.-P. Bucher, and K. Kern, Nature (London) **366**, 141 (1993).

[29] V. Musolino, A. Selloni, and R. Car, Phys. Rev. Lett. **83**, 3242 (1999).